

# Multiple regulation by external ATP of nifedipine-insensitive, high voltage-activated $\text{Ca}^{2+}$ current in guinea-pig mesenteric terminal arteriole

Hiromitsu Morita, Thapaliya Sharada\*, Tadashi Takewaki\*, Yushi Ito and Ryuji Inoue

Department of Pharmacology, Graduate School of Medical Sciences, Kyushu University, Fukuoka 812-8582, Japan and the \* United Graduate School of Veterinary Science, Gifu University, Gifu 501-1193, Japan

We investigated the receptor-mediated regulation of nifedipine-insensitive, high voltage-activated  $\text{Ca}^{2+}$  currents in guinea-pig terminal mesenteric arterioles ( $I_{\text{mVDCC}}$ ) using the whole-cell clamp technique. Screening of various vasoactive substances revealed that ATP, histamine and substance P exert modulatory effects on  $I_{\text{mVDCC}}$ . The effects of ATP on  $I_{\text{mVDCC}}$  after complete P2X receptor desensitization exhibited a complex concentration dependence. With 5 mM  $\text{Ba}^{2+}$ , ATP potentiated  $I_{\text{mVDCC}}$  at low concentrations ( $\sim 1\text{--}100 \mu\text{M}$ ), but inhibited it at higher concentrations ( $>100 \mu\text{M}$ ). The potentiating effects of ATP were abolished by suramin (100  $\mu\text{M}$ ) and PPADS (10  $\mu\text{M}$ ) and by intracellular application of  $\text{GDP}\beta\text{S}$  (500  $\mu\text{M}$ ), whereas a substantial part of  $I_{\text{mVDCC}}$  inhibition by millimolar concentrations of ATP remained unaffected; due probably to its divalent cation chelating actions. In divalent cation-free solution,  $I_{\text{mVDCC}}$  was enlarged and underwent biphasic effects by  $\text{ATP}\gamma\text{S}$  and ADP, while 2-methylthio ATP (2MeSATP) exerted only inhibition, and pyrimidines such as UTP and UDP were ineffective. ATP-induced  $I_{\text{mVDCC}}$  potentiation was selectively inhibited by anti- $\text{G}\alpha_s$  antibodies or protein kinase A (PKA) inhibitory peptides and mimicked by dibutyryl cAMP. In contrast, ATP-induced inhibition was selectively inhibited by  $\text{G}\alpha_{q/11}$  antibodies or protein kinase C (PKC) inhibitory peptides and mimicked by PDBu. Pretreatment with pertussis toxin was ineffective. The apparent efficacy for  $I_{\text{mVDCC}}$  potentiation with PKC inhibitors was:  $\text{ATP}\gamma\text{S} > \text{ATP} \geq \text{ADP}$  and for inhibition with PKA inhibitors was:  $2\text{MeSATP} > \text{ATP}\gamma\text{S} > \text{ATP} > \text{ADP}$ . Neither  $I_{\text{mVDCC}}$  potentiation nor inhibition showed voltage dependence. These results suggest that  $I_{\text{mVDCC}}$  is multi-phasically regulated by external ATP via  $\text{P2Y}_{11}$ -resembling receptor/ $\text{G}_s$ /PKA pathway,  $\text{P2Y}_1$ -like receptor/ $\text{G}_{q/11}$ /PKC pathway, and metal chelation.

(Received 23 July 2001; accepted after revision 20 December 2001)

**Corresponding author** R. Inoue: Department of Pharmacology, Graduate School of Medical Sciences, Kyushu University, Fukuoka 812-8582, Japan. Email: inouery@pharmaco.med.kyushu-u.ac.jp

Voltage-dependent  $\text{Ca}^{2+}$  channels (VDCCs) serve as a main potential-dependent  $\text{Ca}^{2+}$  entry pathway in a wide range of tissues and have been implicated in a variety of cellular processes such as muscle contraction, neurotransmitter release, cell proliferation and development (Bean, 1989a). Several distinct classes of VDCCs have been identified on a biophysical and pharmacological bases (L-, N-, P/Q-, T-, R-type), and subsequently, ten  $\alpha_1$ -subunit encoding genes responsible for these phenotypes have been cloned ( $\alpha_{1A-I}$  and  $\alpha_{1S}$ ; Davila, 1999; Hofmann *et al.* 2000). Amongst them, the dihydropyridine-sensitive, L-type VDCC has been found ubiquitously over the whole vasculature and is thought to play a crucial role in the control of blood flow and pressure (Nelson *et al.* 1990). However, it has recently been reported that, in the peripheral branches of the mesenteric arterial tree (or higher-ordered arterioles), the predominant VDCC is a class of high voltage-activated (HVA) channels, the properties of which do not match up with those of hitherto-known

VDCCs (Morita *et al.* 1999; hereafter designated as mVDCC). In addition to its unique biophysical properties, the mVDCC is totally insensitive to known blockers for L-, N-, P/Q-, T- and R-type VDCCs such as nifedipine, verapamil, diltiazem,  $\omega$ -conotoxins GVIA and MVIIC, and  $\omega$ -agatoxin IVA (Morita *et al.* 1999), thus presumably belonging to a new class of HVA-VDCC that has not yet been characterized at the molecular level.

Detailed electrophysiological analysis of mVDCC has revealed that, despite its rapidly inactivating nature, there is a range of membrane potential in which constant or non-inactivating  $\text{Ca}^{2+}$  influx occurs. The physiological significance of non-inactivating  $\text{Ca}^{2+}$  influx has been emphasized for L-type VDCC, as the critical determinant of free  $\text{Ca}^{2+}$  concentration ( $[\text{Ca}^{2+}]_i$ ) in arterial smooth muscle cells and thus of the arterial diameter or tone under pressurized conditions (for review see Nelson *et al.* 1990). Furthermore, this  $\text{Ca}^{2+}$  influx has been thought to be effectively regulated by the modulatory actions of various

vasoactive substances such as neurotransmitters (e.g. noradrenaline, neuropeptide Y, acetylcholine, vasointestinal peptide and calcitonin gene-related peptide), vasoactive autacoids which are released from the vascular endothelium or produced during local inflammatory processes (e.g. nitric oxide, endothelium-derived hyperpolarizing factor, endothelin, histamine and bradykinin) and circulating hormones released from distant endocrine organs (e.g. angiotensin II and vasopressin) (Beech, 1998; Kuriyama *et al.* 1998).

In the present study, we have therefore addressed the question of whether receptor-mediated regulation has a similar physiological significance in modifying the mVDCC activity. To this end, we screened the effects on mVDCC of vasoactive substances known to affect the electrical and contractile properties of vascular smooth muscle. We have found that ATP, a well established fast neurotransmitter of the vascular sympathetic nerves (Burnstock, 1990), exerts the most pronounced dose-dependent modulatory effects on mVDCCs through three distinct mechanisms. The preliminary account of this work has been presented in the 73rd annual meeting of the Japanese Pharmacological Society (Morita *et al.* 2000).

## METHODS

### Cell dispersion and electrophysiological measurements

Procedures used for cell dispersion and the system for patch clamp experiments were the same as described previously (Morita *et al.* 1999) and performed according to the guidelines approved by a local animal ethics committee of Kyushu University. In brief, guinea-pigs of either sex weighing 200–500 g were killed by decapitation after stunning under light anaesthesia with inhalation of diethyl ether. Short segments from the distal half of terminal branches of mesenteric artery measuring 70–100  $\mu\text{m}$  in diameter were mechanically dissected with fine scissors and forceps, and incubated successively in nominally  $\text{Ca}^{2+}$ -free Krebs solutions without and with 2 mg  $\text{ml}^{-1}$  collagenase (Sigma type I) at 35°C for 30 and 60 min, respectively. Single cells, yielded by gently triturating these digested segments using a blunt tipped pipette 20 to 30 times, were stored in 0.5 mM  $\text{Ca}^{2+}$ -containing Krebs solution at 10°C until use.

A commercial amplifier (Axopatch 1D, Axon Instruments) in conjunction with an A/D, D/A converter was used to generate voltages and sample current signals after low-pass filtering at 1 kHz (digitized at 2 kHz), under the control of an IBM computer (Aptiva) which was driven by a commercial software Clampex v.6.02 (Axon Instruments). The P/4 or P/2 method was used to subtract leak currents, and 50 to 70% of series resistance (10–15 M $\Omega$ ) was electronically compensated. Data analyses and illustration were performed using Clampfit v.6.02 (Axon Instruments). All experiments were performed at room temperature (22–25°C).

### Solutions

Solutions of the following composition were used (mM): 5  $\text{Ba}^{2+}$ -external solution:  $\text{Na}^+$  140,  $\text{K}^+$  6,  $\text{Ba}^{2+}$  5,  $\text{Mg}^{2+}$  1.2,  $\text{Cl}^-$  158.4, glucose 10, Hepes 10 (pH 7.4; adjusted by Tris base); divalent cation-free external solution:  $\text{Na}^+$  140,  $\text{K}^+$  6,  $\text{Cl}^-$  146, EDTA 0.2,

glucose 10, Hepes 10 (pH 7.4; adjusted by Tris base). All external solutions were supplemented with nifedipine 10  $\mu\text{M}$  and were superfused at a rate of 1–2  $\text{ml min}^{-1}$  into the recording chamber (volume  $\sim$ 0.2 ml), via a gravity-fed perfusion system (time of complete solution change  $\sim$ 30 s);  $\text{Cs}^+$ -internal solution:  $\text{Cs}^+$  140,  $\text{Mg}^{2+}$  2,  $\text{Cl}^-$  144, phosphocreatine 5,  $\text{Na}_2\text{ATP}$  1, GTP 0.2, EGTA 10, Hepes 10 (pH 7.2; adjusted by Tris base).

Free ATP and  $\text{Ba}^{2+}$  concentrations (Fig. 3) were calculated using Fabiato and Fabiato's program with enthalpic and ionic strength corrections (Brooks & Storey, 1992) using association constants for  $\text{Ba}^{2+}$  of  $10^{3.29}$  and  $10^{5.1}$ , as performed previously (Inoue & Ito, 2000).

### Chemicals

The following agents were purchased; angiotensin II, bradykinin, calcitonin gene-related peptide, endothelin-1, histamine, neurokinin A & B, neuropeptide Y, neurotensin, somatostatin, substance P, vasointestinal peptide, vasopressin, ADP, AMP, adenosine,  $\alpha,\beta$ -methylene ATP, ATP $\gamma\text{S}$ , AMP-PNP, 2MeSATP, GDP $\beta\text{S}$ , GTP $\gamma\text{S}$ , suramin, PPADS (pyridoxalphosphate-6-azophenyl 2',4'-disulphonic acid), protein kinase A inhibitory peptide (PKI 14–22 amide), protein kinase C inhibitory peptide (PKC 19–31), G-protein  $\alpha$ -subunit antibodies (anti-G $\alpha_s$  and anti-G $\alpha_{q/11}$ ) and pertussis toxin from Calbiochem; acetylcholine, noradrenaline, dibutyryl cAMP, SNAP (S-nitroso-N-acetyl penicillamine) from Sigma; ATP, EDTA and EGTA from Dojin (Kumamoto, Japan). Inhibitors were added into the bath at least 5 min, or intracellularly dialysed via the patch pipette for 10–20 min, before application of test agonists.

### Statistics

All data are expressed as means  $\pm$  s.e.m. To evaluate statistical significance of difference between a given set of data, Student's paired and unpaired *t* tests and one way ANOVA with pooled variance *t* test were employed.

## RESULTS

### External ATP exhibits dual actions on mVDCC

We first investigated the effects of various vasoactive agents known to affect the electrical and contractile responses of vascular smooth muscle (Beech, 1998), on the current flowing through mVDCC ( $I_{\text{mVDCC}}$ ) evoked by 100 ms depolarizing pulses to 0 mV at an interval of 20 s from a holding potential of  $-60$  mV, with 5 mM  $\text{Ba}^{2+}$  as the charge carrier (10  $\mu\text{M}$  nifedipine present). Under these ionic conditions, the amplitude of  $I_{\text{mVDCC}}$  was almost tripled compared with that at physiological concentrations of  $\text{Ca}^{2+}$  (1–2 mM), without significant changes in the voltage-dependent properties or contamination of other  $\text{Ca}^{2+}$ -dependent conductances (Morita *et al.* 1999). The majority of the vasoactive agents tested (5–10 min application;  $n = 3$ –6) failed to affect  $I_{\text{mVDCC}}$  at the sub-maximally or maximally effective concentrations reported to modulate L-type VDCCs (Beech, 1998). These include calcitonin gene-related peptide (100 nM), acetylcholine (1  $\mu\text{M}$ ), vasointestinal peptide (1  $\mu\text{M}$ ), noradrenaline (10  $\mu\text{M}$ ), neuropeptide Y (1  $\mu\text{M}$ ), endothelin-1 (1  $\mu\text{M}$ ), angiotensin II (1  $\mu\text{M}$ ), vasopressin (1  $\mu\text{M}$ ), neurokinin A and B (each 1  $\mu\text{M}$ ), neurotensin (1  $\mu\text{M}$ ), somatostatin

(1  $\mu\text{M}$ ), bradykinin (10  $\mu\text{M}$ ) and the nitric oxide-releasing agent, SNAP (100  $\mu\text{M}$ ). In contrast, significant potentiation (10  $\mu\text{M}$ ;  $119 \pm 3\%$  of control,  $n = 5$ ) and inhibition (10 mM;  $33 \pm 2\%$  of control,  $n = 5$ ) of  $I_{\text{mVDCC}}$  occurred with externally applied ATP in a dose-dependent fashion. Modest inhibition was also observed for substance P (1  $\mu\text{M}$ ;  $77 \pm 2\%$  of control,  $n = 5$ ) and histamine (10  $\mu\text{M}$ ;  $90 \pm 2\%$  of control,  $n = 4$ ). Since ATP is an established major neurotransmitter of vascular sympathetic nerves and is responsible for generating the fast excitatory junction potential (EJP) in the mesenteric arterioles (Starke, 1991;

Thapaliya *et al.* 1999), we concentrated on investigating the effects of ATP in the rest of this study.

### Three mechanisms involved in ATP actions

Figure 1A illustrates a typical time course of the effects of ATP on  $I_{\text{mVDCC}}$  (filled circles) and the holding current under voltage clamp at  $-60$  mV. Immediately after addition of 100  $\mu\text{M}$  ATP in the bath, a rapidly growing and desensitizing inward current was activated, and subsequently, the magnitude of  $I_{\text{mVDCC}}$  gradually increased. The rapidly desensitizing inward current is likely to be

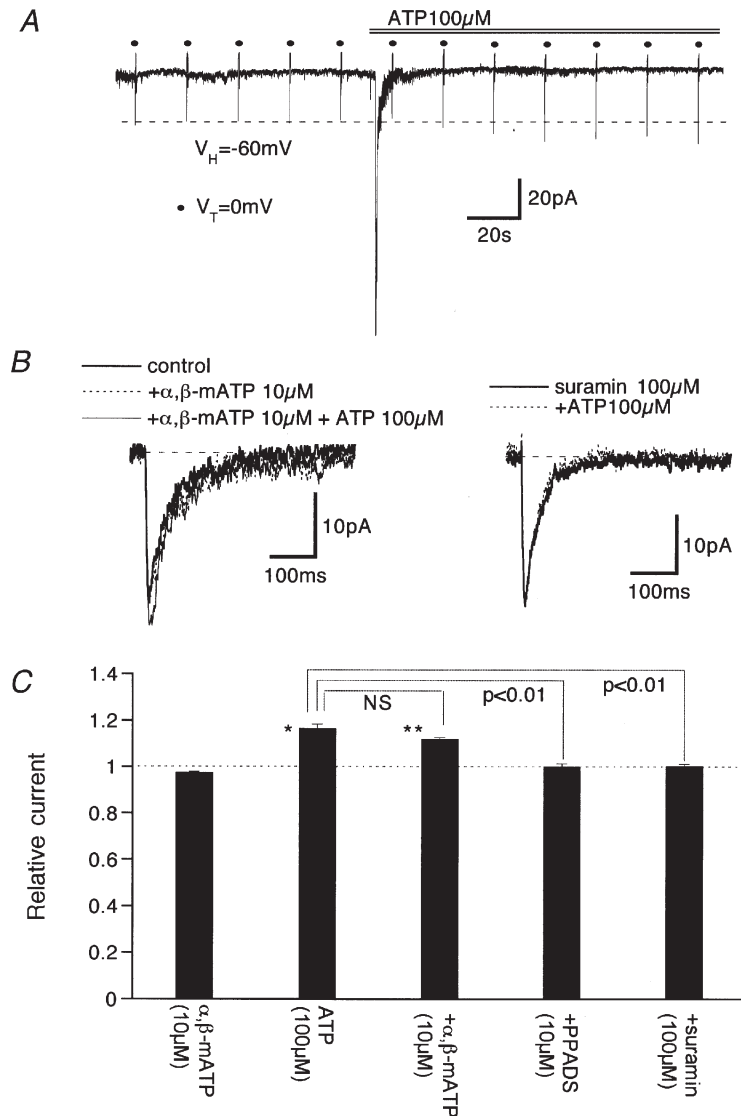


**Figure 1. The effects of ATP and purnergic receptor antagonists on  $I_{\text{mVDCC}}$**

Bath and pipette contained 5 mM Ba<sup>2+</sup> external and Cs<sup>+</sup> internal solutions, respectively. A, time course of the effects of 100  $\mu\text{M}$  ATP on  $I_{\text{mVDCC}}$  (●) and holding current. 100 ms depolarizing pulses to 0 mV ( $V_{\text{T}}$ ) from a holding potential of  $-60$  mV ( $V_{\text{H}}$ ) were applied at an interval of 20 s. B, leak-subtracted traces of  $I_{\text{mVDCC}}$  in the presence of 10  $\mu\text{M}$   $\alpha, \beta$ -methylene ATP ( $\alpha, \beta$ -mATP, left) or 100  $\mu\text{M}$  suramin (right) with or without 100  $\mu\text{M}$  ATP. C, summary of the effects of pretreatment with  $\alpha, \beta$ -mATP (10  $\mu\text{M}$ ), PPADS (10  $\mu\text{M}$ ) and suramin (100  $\mu\text{M}$ ) on ATP (100  $\mu\text{M}$ )-induced potentiation of  $I_{\text{mVDCC}}$ . Columns and bars indicate means  $\pm$  s.e.m. from 4–5 experiments. \*, \*\* Statistically significant difference ( $P < 0.05$  and 0.01, respectively) from the control value (dotted line). NS (not significant) and  $P$  values in the figure indicate the results of one way ANOVA and pooled variance  $t$  test.

the non-selective cationic current of P2X receptor (Surprenant *et al.* 1995) and responsible for the fast EJP in the present preparation. This is suggested by the observation that pretreatment with  $\alpha,\beta$ -methylene ATP (10  $\mu\text{M}$ ) or total substitution of external cations with a large impermeant cation *N*-methyl, *D*-glucamine completely abolished both the inward current and the EJPs (data not shown). In contrast, potentiation of  $I_{\text{mVDCC}}$  by 100  $\mu\text{M}$  ATP persisted over several minutes and was strongly suppressed by pretreatment with the P2 receptor antagonists, PPADS or suramin (Fig. 1B and C; Fig. 2) but not affected by  $\alpha,\beta$ -methylene ATP (Fig. 1B and C). These results indicate that the non-P2X receptors are involved in the potentiation of  $I_{\text{mVDCC}}$ .

Significant potentiation of  $I_{\text{mVDCC}}$  by ATP occurred at a concentration as low as 1  $\mu\text{M}$ , with the maximum response between 10 and 100  $\mu\text{M}$ . However, at higher concentrations of ATP (>100  $\mu\text{M}$ ), the potentiating effect declined and was ultimately converted to pronounced inhibition in the millimolar range (filled circles in Fig. 2). ATP-induced  $I_{\text{mVDCC}}$  potentiation in the micromolar range disappeared when 500  $\mu\text{M}$  GDP $\beta$ S instead of GTP was included in the pipette (open circles in Fig. 2). However, the inhibition in the millimolar range remained almost unaffected with this procedure (dashed line in Fig. 2). These results strongly suggest that ATP-induced  $I_{\text{mVDCC}}$  potentiation involves activation of the P2Y receptor/G-protein pathway, whereas inhibition in the millimolar ATP range may result from a mechanism independent of receptor activation, i.e. reduced  $\text{Ba}^{2+}$  concentration due to the chelating action of ATP (see below).

In order to eliminate a possible interaction between ATP and divalent cations and also to examine the effects of ATP with a better signal-to-noise ratio, we next recorded  $I_{\text{mVDCC}}$  using  $\text{Na}^+$  as the charge carrier under divalent cation-free conditions (200  $\mu\text{M}$  EDTA added in the bath). Under these conditions, the amplitude of  $I_{\text{mVDCC}}$  was increased 20–40 times and was dependent on the  $\text{Na}^+$  concentration in the bath, but insensitive to tetrodotoxin (10  $\mu\text{M}$ ) and was completely blocked by micromolar concentrations of  $\text{Cd}^{2+}$  (Fig. 3A and B). The current–voltage relationship of  $I_{\text{mVDCC}}$  was shifted negatively by about 20 mV (data not shown).

As summarized in Fig. 3C, the relationship between ATP concentration and the amplitude of the  $\text{Na}^+$  current through mVDCC channels was shifted to the left by about two logarithmic scales, as compared with that obtained when  $\text{Ba}^{2+}$  was the charge carrier (Fig. 2), although marked inhibition of  $I_{\text{mVDCC}}$  in a very high ATP concentration range disappeared due probably to virtual absence of  $\text{Na}^+$  chelation by ATP. This can be interpreted as indicating that the free form of ATP is responsible for its effects on  $I_{\text{mVDCC}}$ . In support of this idea, re-scaling the abscissa of dose–response data with 5 mM  $\text{Ba}^{2+}$  solution (Fig. 2) with respect to the free ATP concentration gave a comparable concentration dependence to that observed under divalent cation-free conditions (Fig. 3C). Interestingly, in the micromolar range of ATP (>1  $\mu\text{M}$ ), the potentiating effect turned to a clear decline as the concentration of ATP was increased, and substantial inhibition of  $I_{\text{mVDCC}}$  occurred at concentrations of 1 mM or higher (Fig. 3C). This inhibition could not result from  $\text{Na}^+$  chelation by ATP (1 mM ATP would cause only ~0.4% reduction in  $\text{Na}^+$

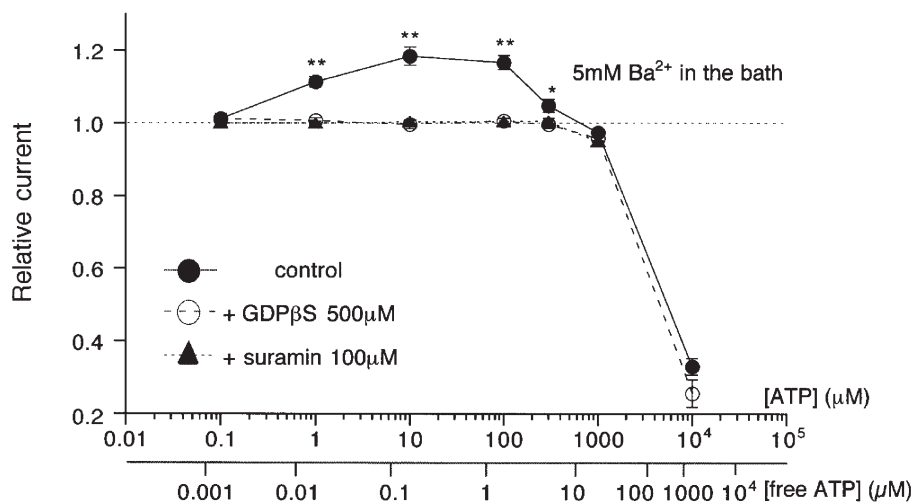


**Figure 2. Concentration-dependent profile of ATP effects on  $I_{\text{mVDCC}}$  with 5 mM  $\text{Ba}^{2+}$  as the charge carrier**

Recording conditions were the same as in Fig. 1. ● and ○, and ▲ indicate the amplitude of  $I_{\text{mVDCC}}$  relative to that before addition of ATP, in the absence and presence of 500  $\mu\text{M}$  GDP $\beta$ S in the pipette or 100  $\mu\text{M}$  suramin (pretreated for 5 min) in the bath. The effects of ATP were monitored for at least 5 min and the maximum effects were taken. The scale in the lower abscissa (free ATP concentration) was calculated as described in Methods. \*, \*\* Statistically significant difference ( $P < 0.05$  and 0.01, respectively) between ● and ○ at each ATP concentration with unpaired *t* test, respectively.

concentration), and seems to correspond to the decline of potentiation observed in the high micromolar range of ATP ( $100 \mu\text{M}$  to  $1 \text{ mM}$ ) with  $\text{Ba}^{2+}$  as the charge carrier (Fig. 2). The inhibition was more clearly manifested when the potentiating effect was selectively eliminated (see below), and it is likely that a P2Y receptor/G-protein pathway is also involved, since the inhibition was completely abolished when  $\text{GDP}\beta\text{S}$  (open circles in Fig. 3C) was present in the pipette or P2 antagonists such as suramin and PPADS were added to the bath (not shown).

### Two distinct P2Y receptors regulate mVDCC

The P2Y receptors can be pharmacologically distinguished based on the relative potencies of purines and pyrimidines (Kunapuli & Daniel, 1998; King *et al.* 1998). We therefore compared the potencies of various purines and pyrimidines

for potentiating and inhibiting  $I_{\text{mVDCC}}$ . As summarized in Fig. 4, ADP exhibited concentration-dependent effects on  $I_{\text{mVDCC}}$  similar to ATP, while AMP and adenosine were ineffective (data not shown). This could suggest that the ATP effects seen were subsequent to its degradation to ADP. However, this possibility is unlikely, since a slowly hydrolysable ATP analogue,  $\text{ATP}\gamma\text{S}$ , also exhibited a comparable efficacy to ATP in both potentiating and inhibiting  $I_{\text{mVDCC}}$ . We also tested another purine, 2MeSATP, and pyrimidines such as UDP and UTP. While 2MeSATP caused only a dose-dependent inhibition of  $I_{\text{mVDCC}}$ , UDP or UTP did not exert any discernible effects.

These pharmacological profiles strongly suggest that there are at least two distinct P2Y receptor/G-protein pathways involved in potentiation and inhibition of  $I_{\text{mVDCC}}$  (see Discussion).

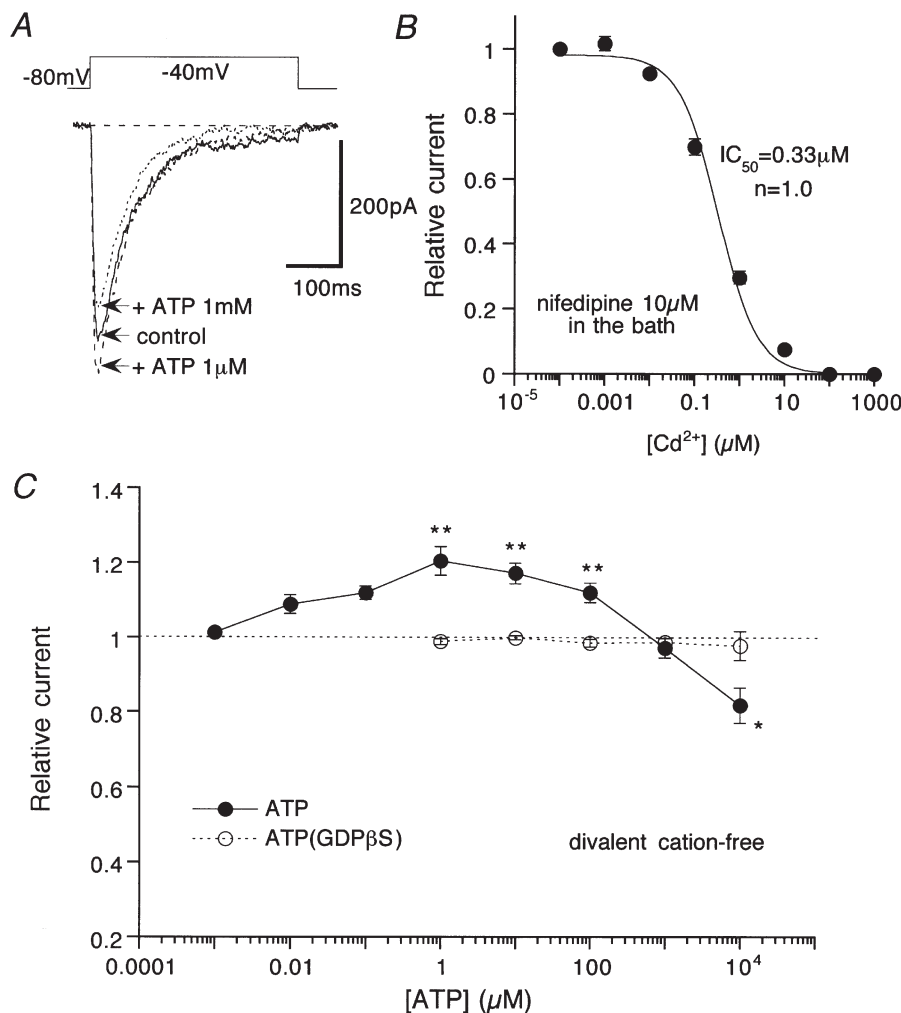


**Figure 3. Concentration-dependent effects of ATP on  $I_{\text{mVDCC}}$  with  $\text{Na}^+$  as the charge carrier (divalent cation-free conditions)**

Nifedipine ( $10 \mu\text{M}$ ) in the bath. *A*, actual traces of  $I_{\text{mVDCC}}$  (leak-subtracted). Uppermost trace indicates the waveform of the step pulses used. *B*,  $\text{Cd}^{2+}$  concentration–inhibition curve for  $I_{\text{mVDCC}}$ . ● and bars represent means  $\pm$  s.e.m. from 5 cells and the smooth continuous curve is the result of Hill fitting. *C*, relationship between ATP concentration and the  $I_{\text{mVDCC}}$  amplitude. ● and ○, mean of data pooled from 5–20 cells in the absence and presence of  $500 \mu\text{M}$   $\text{GDP}\beta\text{S}$  in the pipette, respectively. \*  $P < 0.05$  and \*\*  $P < 0.01$  with Student's unpaired *t* test for the ATP concentration data (● and ○).

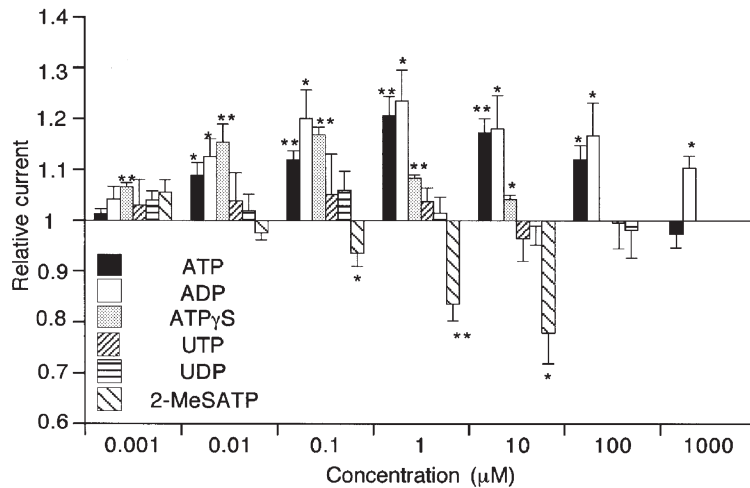
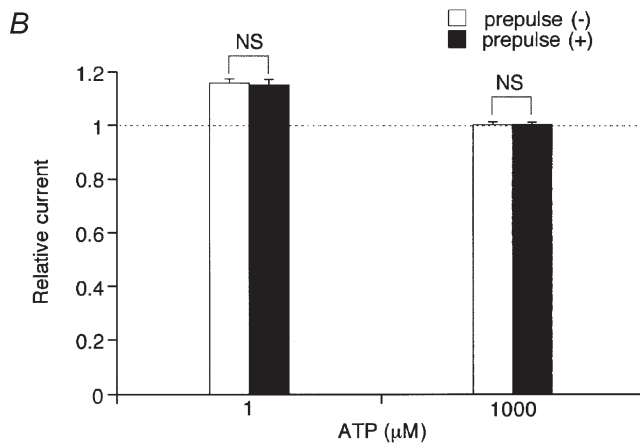
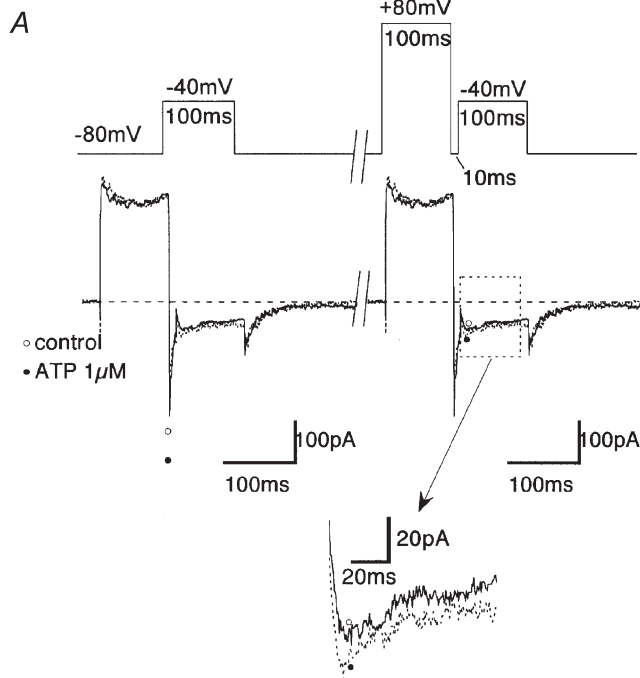


**Figure 4. Effects of various nucleotides on  $I_{mVDCc}$  evaluated with  $Na^+$  as charge carrier (divalent cation-free conditions)**

Nifedipine ( $10 \mu M$ ) in the bath. Voltage step pulses (100 ms: from  $-80$  to  $-40$  mV) were used to evoke  $I_{mVDCc}$ . \*  $P < 0.05$  and \*\*  $P < 0.01$  with  $t$  test for paired data ( $n = 5-20$ ) before and after application, respectively, of a given nucleotide at a given concentration.



### Involvement of two distinct G-proteins and protein kinases in ATP actions

It has been reported that G-protein-mediated modulation of VDCCs involves both direct interaction with G-protein and phosphorylation/dephosphorylation of VDCC proteins (Bean, 1989b; Dolphin, 1998; Hofmann *et al.* 1999). However, the former mechanism seems unlikely to account for the observed effects of ATP on  $I_{mVDCc}$ . As demonstrated in Fig. 5A, large depolarizing prepulses, which were used to relieve G-protein-mediated inhibition (N- or P/Q-type VDCCs; Dolphin, 1998; Kaneko *et al.* 1999), merely facilitated the voltage-dependent inactivation of  $I_{mVDCc}$ , and did not significantly alter the extent of either ATP-induced potentiation or inhibition of  $I_{mVDCc}$  (Fig. 5B). In contrast, inclusion of protein kinase A and C inhibitory peptides in the pipette selectively abolished the ATP-induced potentiation and inhibition of  $I_{mVDCc}$ , respectively (open and shaded columns in Fig. 6A), and the simultaneous inclusion of both peptides almost completely abolished the effects of ATP (hatched column in Fig. 6A). The  $EC_{50}$  and  $IC_{50}$  values for ATP-induced  $I_{mVDCc}$  potentiation and inhibition evaluated under these conditions are about  $10 \text{ nM}$  and  $>10 \mu M$ , respectively (Fig. 6A; see also Fig. 7). Consistent with these observations, bath application of dibutyryl cAMP ( $1 \text{ mM}$ ), which is a membrane permeable cAMP analogue and directly activates PKA bypassing the

### Figure 5. Large preceding depolarization does not affect the extent of ATP-induced $I_{mVDCc}$ potentiation and inhibition

A, voltage protocol (upper trace) and corresponding current traces before (○ and continuous curve) and after (● and dotted curve) addition of  $1 \mu M$  ATP. Inset indicated by arrow is magnification from a part boxed by dotted line. B, relative amplitude change of  $I_{mVDCc}$  after addition of  $1 \mu M$  (left) or  $1 \text{ mM}$  (right) ATP with (□) or without (■) a 100 ms prepulse to 80 mV. Experiments carried out with  $Na^+$  as charge carrier (divalent cation-free conditions) in the presence of  $10 \mu M$  nifedipine in the bath. NS, no statistically significant difference with unpaired  $t$  test.  $n = 4$ .

receptor, enhanced, whereas that of PKC activator PDBu (250 nM) suppressed,  $I_{mVDCC}$  (Fig. 6B).

It is generally thought that receptor-mediated activation of PKA and PKC is mediated through their specific subtypes of G-protein,  $G_s$  and  $G_{q/11}$ , respectively. We therefore examined whether antibodies against these G-protein subtypes counteract the ability of ATP to potentiate or inhibit  $I_{mVDCC}$ . As summarized in Fig. 6C, 10–20 min intracellular application of  $G\alpha_s$ -specific antibody via the patch pipette abolished the potentiating effect but not the inhibitory effect of ATP (open columns in Fig. 6C), and vice versa with  $G\alpha_{q/11}$ - instead of  $G\alpha_s$ -specific antibody (shaded columns in Fig. 6C). Simultaneous application of the two antibodies resulted in total abolition of the effects of ATP (hatched columns in Fig. 6C). In addition, overnight pretreatment of mesenteric arteriolar myocytes

with pertussis toxin did not significantly alter the effects of ATP, thus excluding the involvement of  $G_i/G_o$  subtypes in the effects of ATP (Fig. 6D). These results collectively suggest that ATP-induced potentiation and inhibition of  $I_{mVDCC}$  primarily involve activation of the  $P2Y/G_s/PKA$  and  $P2Y/G_{q/11}/PKC$  pathways, respectively.

The sequence of efficacy of nucleotides to cause  $I_{mVDCC}$  potentiation was determined under the conditions in which inhibition via the  $G_{q/11}/PKC$  pathway was selectively eliminated by the PKC inhibitory peptide. As shown in Fig. 7A,  $K_d$  values evaluated by Hill fitting suggest that this sequence is  $ATP\gamma S > ATP \geq ADP$ . Similarly, with the PKA inhibitory peptide for eliminating  $I_{mVDCC}$  potentiation, the nucleotide sequence to inhibit  $I_{mVDCC}$  is  $2MeSATP > ATP\gamma S > ATP > ADP$  (Fig. 7B).

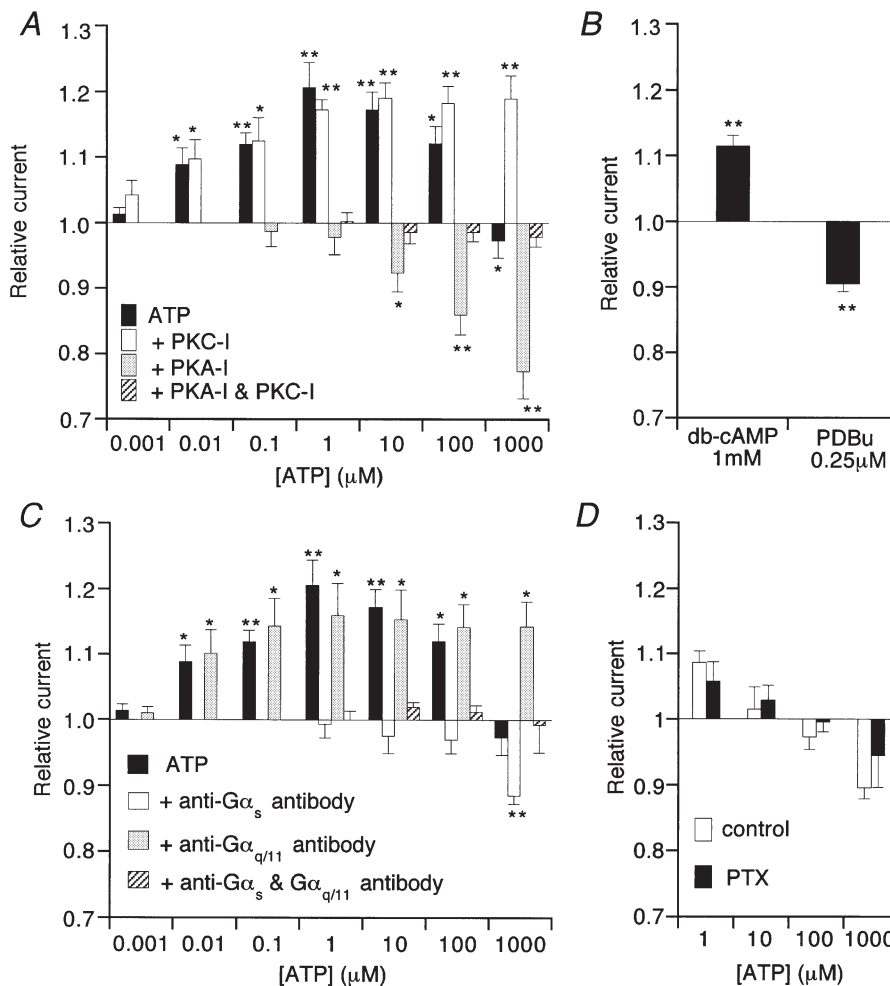


**Figure 6. Effects of protein kinase inhibitors (A) activators (B), G-protein antibodies (C) and overnight pertussis toxin treatment (D) on ATP-induced modulation of  $I_{mVDCC}$**

Recording conditions were the same as in Fig. 4. PKC-I, protein kinase C inhibitory peptide (1 μM); PKA-I, protein kinase A inhibitory peptide (41.3 nM); PTX, pertussis toxin. In C, antibodies against  $G\alpha_s$  and  $G\alpha_{q/11}$  were diluted 1:35 in the pipette solution. In D, mesenteric arteriolar myocytes were incubated with (PTX) or without (control) pertussis toxin (500 ng ml<sup>-1</sup>) at 10°C for 24h. \* $P < 0.05$  and \*\* $P < 0.01$  with  $t$  test for paired data ( $n = 5$ ) before and after application of a given concentration of ATP, dbcAMP or PDBu.

**Table 1 Comparison of nucleotide sensitivity of various P2Y receptors**

Subtype	P2Y <sub>1</sub>	P2Y <sub>2</sub>	P2Y <sub>4</sub>	P2Y <sub>6</sub>	P2Y <sub>11</sub>	P2Y <sub>12</sub>	P2Y <sub>(pot)</sub>	P2Y <sub>(inh)</sub>
G-protein	G <sub>q/11</sub>	G <sub>q/11</sub>	G <sub>q/11</sub>	G <sub>q/11</sub>	G <sub>s</sub> ,G <sub>q/11</sub>	G <sub>i/o</sub>	G <sub>s</sub>	G <sub>q/11</sub>
Coupling	PLC β/IP <sub>3</sub> ↑	PLC β/IP <sub>3</sub> ↑	PLC β/IP <sub>3</sub> ↑	PLC β/IP <sub>3</sub> ↑	PLC β/IP <sub>3</sub> ↑ AC/cAMP↑	AC/cAMP↓	AC/cAMP↑	PLC β/IP <sub>3</sub> ↑ (DAG/PKC)
<i>Antagonists</i>								
PPADS(10 μM)	+	-	-	+*	na	-	+	+
suramin(100 μM)	+	+	-	+	+	+	+	+
<i>Agonist sensitivity</i>								
	2MeSATP >>ATP γS >ATP>ADP	UTP>ATP >ATP γS	UTP=ATP	UDP>UTP >>2MeSATP	ATPγS>ATP >2MeSATP	2MeSATP >ADP >>ATPγS	ATPγS> ATP>ADP (MeSATP:NE)	2MeSATP> ATPγS>ATP >ADP

The agonist sensitivity in the second column is determined based on EC<sub>50</sub> values of Jacobson *et al.* (2000). Other information is based on Boarder & Hourani (1998), King *et al.* (1998), Kunapuli & Daniel (1998) and Hollopeter *et al.* (2001). The data in the third column are from the present work. +, effective; +\*, effective at 100 μM; -, ineffective. PLCβ, phospholipase Cβ; IP<sub>3</sub>, inositol 1,4,5-trisphosphate; DAG, diacylglycerol; AC, adenylate cyclase; NE, not effective. Affixes '(pot)' and '(inh)' indicate the potentiation and inhibition of *I*<sub>mVDCC</sub>, respectively, na, not available.

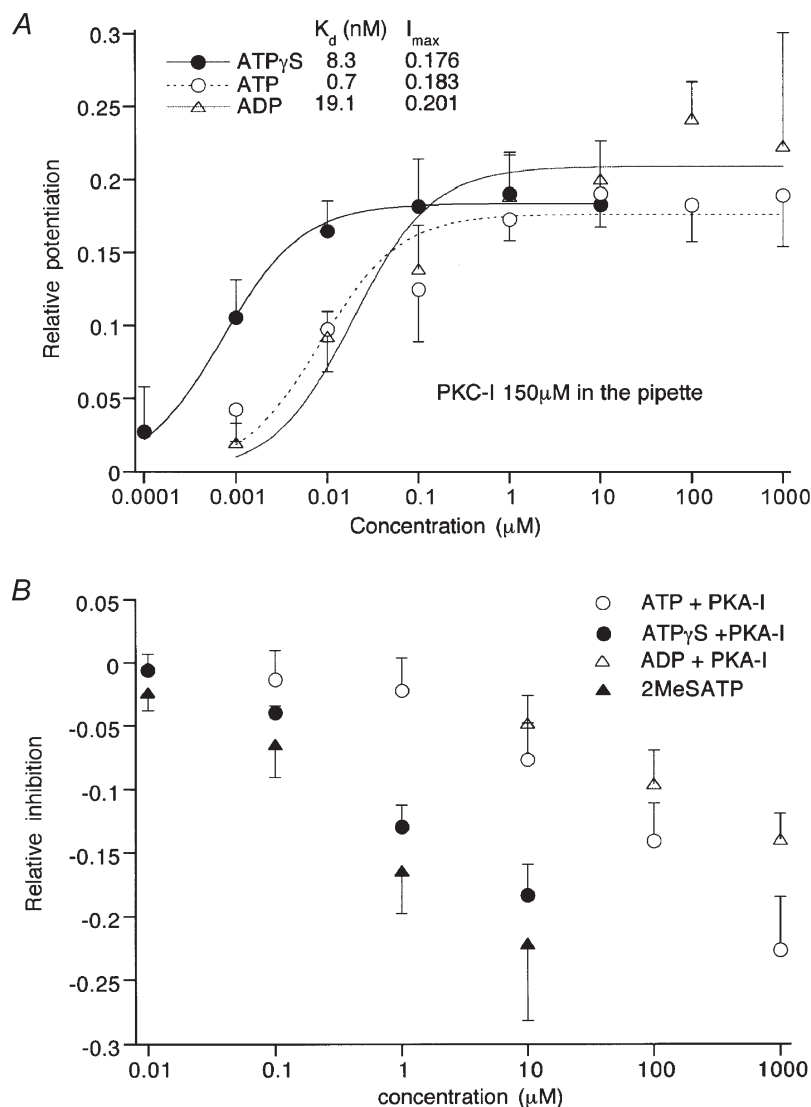


**Figure 7. Efficacies of nucleotides to cause *I*<sub>mVDCC</sub> potentiation (A) and inhibition (B) revealed in the presence of protein kinase inhibitors**

Recording and other experimental conditions were the same as in Fig. 4. A, the extent of *I*<sub>mVDCC</sub> potentiation relative to control is plotted against a given nucleotide concentration. Curves are the results of Hill fitting:  $I_{max}/(1 + K_d/[nucleotide])$ , where  $I_{max}$ ,  $K_d$  and  $[nucleotide]$  denote the maximum potentiation, dissociation constant, and given nucleotide concentration, respectively. B, the extent of *I*<sub>mVDCC</sub> inhibition relative to control is plotted against a given nucleotide concentration. Symbols and vertical bars represent means ± s.e.m. ( $n = 4-6$ ).



**P2Y-mediated modulation of mVDCC shows virtually no alteration of activation and inactivation kinetics**

Finally, to gain more insight into the nature of ATP-induced  $I_{mVDCC}$  modulation, we investigated what changes would occur in the activation and inactivation kinetics of  $I_{mVDCC}$  during application of ATP, using 5 mM Ba<sup>2+</sup> as the charge carrier. As illustrated in Fig. 8A, the shape of the current–voltage relationship of  $I_{mVDCC}$  remained almost unchanged after potentiation by 100 μM ATP, with a similar extent of increase in  $I_{mVDCC}$  amplitude over a wide range of potentials. Correspondingly, there was little discernible shift on application of 100 μM ATP, in either the activation curve for  $I_{mVDCC}$  evaluated by the tail current analysis or the quasi steady-state inactivation curve evaluated by 10 s long conditioning prepulses (Fig. 8B). Similar voltage independent properties were also observed when inhibition of  $I_{mVDCC}$  by higher concentrations of ATP

(1 mM) was separated from potentiation by inclusion of protein kinase A inhibitory peptide in the pipette (Fig. 8C).

These results, together with the absence of voltage-dependent relief, indicate that P2Y receptor-mediated modulation of  $I_{mVDCC}$  occurs through voltage-independent mechanisms which are clearly distinguishable from voltage-dependent receptor-mediated modulation of the other types of dihydropyridine-insensitive, high voltage-activated VDCCs (Dolphin, 1998; Hofmann *et al.* 1999; Kaneko *et al.* 1999).

**DISCUSSION**

The results of the present work clearly show that ATP, but not other potent vasoconstrictors (noradrenaline, angiotensin II and endothelin, etc.), exerts concentration-dependent, triphasic effects on mVDCC activities. In low and high micromolar concentration ranges, ATP caused

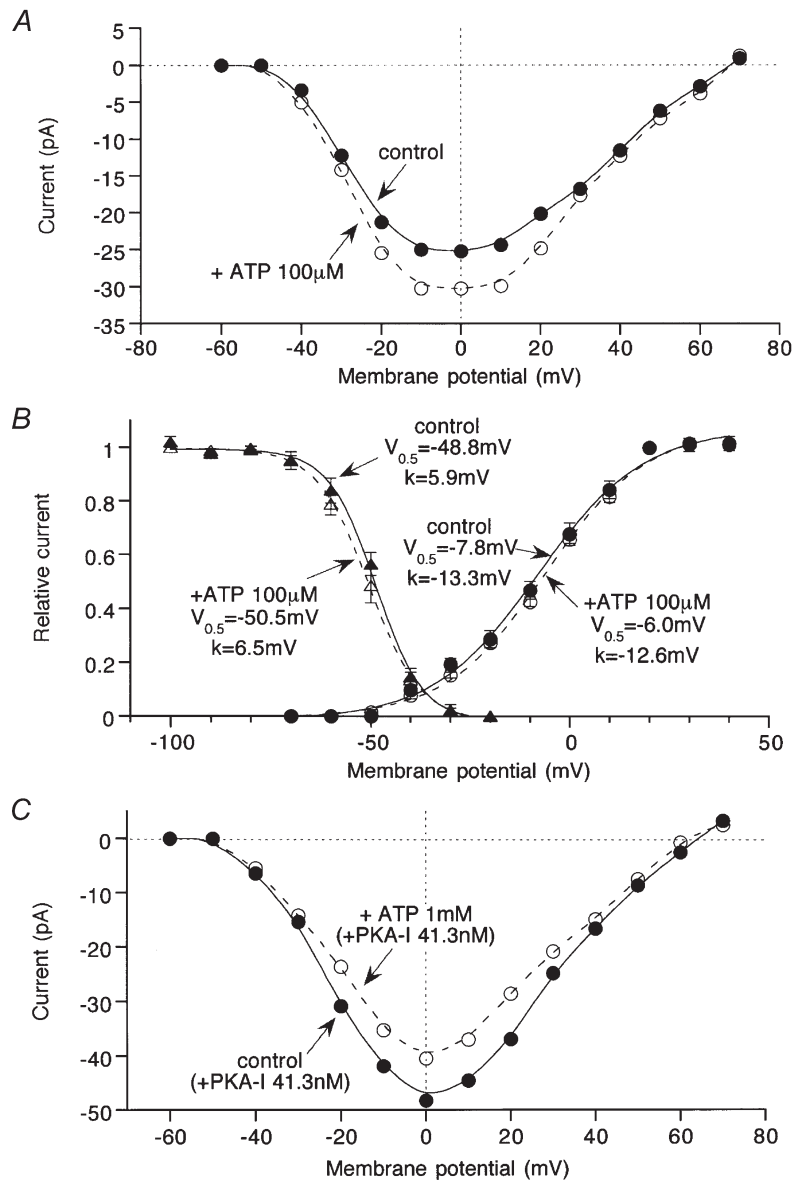
**Figure 8. ATP-induced  $I_{mVDCC}$  potentiation and inhibition is voltage independent**

In order to evaluate the voltage-dependent properties of  $I_{mVDCC}$  under conditions as similar to the physiological situation as possible, Ba<sup>2+</sup> was used as the charge carrier. Bath and pipette contained 5 mM Ba<sup>2+</sup>-external and Cs<sup>+</sup>-internal solutions, respectively. A, current–voltage relationships for  $I_{mVDCC}$  in the absence and presence of 100 μM ATP (A) in the bath. B,  $I_{mVDCC}$  activation curve evaluated by tail current analysis and quasi steady-state inactivation curve evaluated by 10 s preconditioning pulses (see Morita *et al.* 1999). Smooth curves are the best fit of data points ( $n = 5$ ) by Boltzmann equation:

$$1/(1 + \exp((V_m - V_{0.5})/k)),$$

where  $V_m$ ,  $V_{0.5}$  and  $k$  denote membrane potential, half activation or inactivation voltage and slope factor, respectively.

C, current–voltage relationships for  $I_{mVDCC}$  in the absence and presence of 1 mM ATP with 41.3 nM protein kinase A inhibitory peptide in the pipette.



the potentiation and inhibition of  $I_{mVDCC}$  via two distinct G-protein coupled P2Y receptors, while in the millimolar range, it exerted a G-protein-independent inhibition, most likely through divalent cation-trapping actions. These conclusions are supported by the following observations. (1) The first two ATP effects were completely abolished by intracellular application of the G-protein inactivating agent GDP $\beta$  and in the presence of P2 antagonists suramin or PPADS but not by the P2X-selective antagonist  $\alpha,\beta$ -methylene ATP. (2) The third effect was not affected by these agents but was almost completely lost under divalent cation-free conditions. Since ATP is well established as a neurotransmitter released from the sympathetic nerves which densely innervate the peripheral resistant arterioles (Burnstock, 1990; Starke, 1991), this novel regulatory mechanism for mVDCCs by ATP might serve as an effective control of blood pressure and local circulation (see below).

Pharmacological investigation using various P2Y agonists/antagonists and activators/inhibitors for G-proteins and kinases has suggested that the potentiation of  $I_{mVDCC}$  by ATP is likely to involve  $G_s$ /adenylate cyclase/cAMP/PKA-mediated phosphorylation via a pyrimidine-insensitive P2Y receptor subtype having the agonist sensitivity of  $ATP\gamma S > ATP \geq ADP$  (2MeSATP, UTP and UDP are ineffective) (Table 1; Figs 4 and 7). On the other hand, G-protein-dependent inhibition of mVDCCs seems mediated by the  $G_{q/11}$ /PLC  $\beta$ /PKC pathway via a distinct pyrimidine-insensitive P2Y receptor subtype showing an entirely different spectrum of agonist sensitivity,  $2MeSATP > ATP\gamma S > ATP > ADP$  (UTP and UDP are ineffective; Table 1; Figs 4 and 7). Compared with the recombinant P2Y receptors so far identified (Kunapuli & Daniel, 1998; King *et al.* 1998; Jacobson *et al.* 2000), these overall profiles suggest that the P2Y receptors responsible for inhibition of  $I_{mVDCC}$  are most similar to a phosphoinositide turnover-linked receptor, P2Y<sub>1</sub> subtype, and those for potentiation have some degree of similarity to an adenylylase-stimulating receptor, P2Y<sub>11</sub> subtype (Table 1), although involvement of, as yet, unidentified P2Y isoforms cannot completely be excluded (Boeynaems *et al.* 2000).

Recent contractile studies demonstrated that in several different types of vascular smooth muscle, pyrimidines such as UTP and UDP exert strong vasoconstricting actions via the  $G_{q/11}$ /PLC $\beta$ /IP<sub>3</sub> pathway (Rubino & Burnstock, 1996; Lagaud *et al.* 1996; Miyagi *et al.* 1996; Boarder & Hourani, 1998; Mutafova-Yambolieva *et al.* 2000; Horiuchi *et al.* 2001). In support of this, using RT-PCR analysis, mRNA transcripts for pyrimidine-sensitive P2Y<sub>2</sub>, P2Y<sub>4</sub> or P2Y<sub>6</sub> receptor subtypes have been amplified from some arterial smooth muscles (Harper *et al.* 1998; Boarder & Hourani, 1998; Lewis *et al.* 2000). However, in physiological situations, the contribution of pyrimidine receptors to

vasoconstriction is rather uncertain, since it has been shown that with intact endothelium, extraluminally applied UTP and UDP preferentially activate the endothelial P2Y receptors associated with vasodilatation (P2Y<sub>1</sub> or P2Y<sub>2</sub>) and require very high concentrations to produce vasoconstriction (Miyagi *et al.* 1996; Horiuchi *et al.* 2001). In this respect, our present results have highlighted a new important target for the vasomotor control via hitherto-unidentified P2Y receptor subtypes in vascular smooth muscle. It would thus be interesting to see to what extent this mechanism contributes to the control of peripheral vascular resistance or circulation.

### Possible physiological implications

The degree of  $I_{mVDCC}$  potentiation caused by P2Y receptor stimulation was not larger than 20% (~10% with 1  $\mu$ M ATP, and ~20% at 10 and 100  $\mu$ M ATP), which may raise a question as to the physiological contribution of this mechanism to regulating the small arteriolar tone. However, the observed voltage independence of  $I_{mVDCC}$  potentiation (Fig. 8) implies that the magnitude of non-inactivating  $Ca^{2+}$  influx through mVDCCs (several tenths of a pico ampere; Morita *et al.* 1999), which is indicated by the crossover region of the activation and inactivation curves, would also increase to a similar extent in response to P2Y receptor stimulation in the membrane potential range near the resting level (–60 to –30 mV; Fig. 8B). This change in non-inactivating influx might be significant, albeit small, to elevate the intracellular  $Ca^{2+}$  concentration, since the influx would occur continuously into the cell having an extremely small volume of the order of sub-picolitres (Morita *et al.* 1999). In fact, a comparable magnitude of non-inactivating  $Ca^{2+}$  entry through dihydropyridine-sensitive L-type VDCC has been shown to cause a significant elevation in the intracellular  $Ca^{2+}$  concentration ( $[Ca^{2+}]_i$ ) and thus arterial smooth muscle tone (see e.g. Nelson *et al.* 1990). It would therefore be possible to assume a similar role for mVDCCs in the peripheral arterioles. Indeed, our recent preliminary experiments suggest that nifedipine-insensitive but  $Cd^{2+}$ -inhibitable  $[Ca^{2+}]_i$  increases evoked by moderately elevated  $K^+$  concentrations (20–40 mM) were enhanced by 100  $\mu$ M ATP after full P2X receptor desensitization in the same preparation (H. Morita, Y. Ito & R. Inoue, unpublished data). Furthermore, the extent of  $I_{mVDCC}$  potentiation by ATP was even larger (50–60% at 1–10  $\mu$ M) when recorded with nystatin-perforated technique (H. Morita & R. Inoue, unpublished data), and thus the potentiating mechanism by ATP may have more physiological impact on  $[Ca^{2+}]_i$  regulation in small arteriolar cells via  $I_{mVDCC}$  than expected from the present results. Obviously, further studies will be required to determine the relevance of the above-mentioned speculation more unequivocally.

The observed dose–response relationship for ATP with millimolar concentrations of  $Ba^{2+}$  as a charge carrier

(Fig. 2) has indicated that the extent of P2Y-mediated  $I_{mVDCC}$  potentiation increases dose dependently from a threshold of submicromolar and reaches the maximum at several tens of micromolar. At higher concentrations, however, this turned to a gradual decrease due to simultaneous activation of a P2Y-mediated inhibitory mechanism (Fig. 3C), and at extremely high concentrations (>1 mM), to a marked inhibition via a G-protein-independent mechanism (Fig. 2). The concentration of ATP in the vicinity of vascular smooth muscle cells (VSMCs) cannot be precisely estimated due to vigorous degradation by the ecto-ATPase tightly bound to the cell membrane (Kennedy & Leff, 1995; Kunapli & Daniel, 1998), but it has been known that considerable overflow of ATP occurs from the sympathetic nerve terminal by electrical stimulation, which lasts for minutes and evokes smooth muscle contractions or relaxations (e.g. Starke, 1991). Provided that the local concentration of ATP around VSMCs derived from the sympathetic nerve parallels nerve activity, the observed concentration dependence enables us to envisage how the sympathetic nervous system regulates the peripheral resistance arteriolar tone. With the basal sympathetic activity of about one half to two impulses per second (Guyton & Hall, 1996), a weak potentiating effect of ATP, and presumably that of its metabolite ADP, on Ca<sup>2+</sup> entry through mVDCCs would tend to maintain the basal peripheral vascular tone. With moderately increased sympathetic activities, further increase in Ca<sup>2+</sup> influx through mVDCCs via P2Y receptor activation would enhance the vascular tone in proportion to the degree of nerve excitation. However, with excessive sympathetic activity, counteracting mechanisms start to suppress the Ca<sup>2+</sup> influx, initially through P2Y receptors (P2Y<sub>1</sub>-like) and then more potently through the divalent cation chelating action of ATP, leading ultimately to termination of deleterious excessive contractions. Importantly, the apparent ATP concentration range for the latter inhibitory mechanisms (>100 μM) accords with that at which another vasorelaxant mechanism may operate in small resistant arterioles, namely P2Y receptor (P2Y<sub>2</sub>-like)-mediated endothelium-dependent hyperpolarization (Thapaliya *et al.* 1999), suggesting synergistic inhibitory actions. Further studies evaluating the arteriolar tension or diameter more directly such as myography and video imaging will be needed to delineate the roles of these several distinct P2Y receptors in the peripheral vasculature.

## REFERENCES

- BEAN, B. P. (1989a). Class of calcium channels in vertebrate cells. *Annual Review of Physiology* **51**, 367–384.
- BEAN, B. P. (1989b). Neurotransmitter inhibition of neuronal calcium currents by changes in channel voltage dependence. *Nature* **340**, 153–156.
- BEECH, D. J. (1998). Actions of neurotransmitters and other messengers on Ca<sup>2+</sup> channels and K<sup>+</sup> channels in smooth muscle cells. *Pharmacological Therapeutics* **73**, 91–119.
- BOARDER, M. R. & HOURANI, S. M. (1998). The regulation of vascular function by P2 receptors: multiple sites and multiple receptors. *Trends in Pharmacological Sciences* **19**, 99–107.
- BOEYMAEMS, J.-M., COMMUNI, D., SAVI, P. & HERBERT, J.-M. (2000). P2Y receptors: in the middle of the road. *Trends in Pharmacological Sciences* **21**, 1–3.
- BROOKS, S. P. J. & STOREY, K. B. (1992). Bound and determined: a computer program for making buffers of defined ion concentrations. *Analytical Biochemistry* **201**, 119–126.
- BURNSTOCK, G. (1990). Local mechanism of blood flow control by perivascular nerves and endothelium. *Journal of Hypertension* **8**, 95S–106S.
- DAVILA, H. M. (1999). Molecular and functional diversity of voltage-gated calcium channels. *Annals of the New York Academy of Sciences* **868**, 102–117.
- DOLPHIN, A. (1998). Mechanisms of modulation of voltage-dependent calcium channels by G proteins. *Journal of Physiology* **506**, 3–11.
- ERTEL, E. A., CAMPBELL, K. P., HARPOLD, M. M., HOFMANN, F., MORI, Y., PEREZ-REYES, E., SCHWARTZ, A., SNUTCH, T. P., TANABE, T., BIRNBAUMER, L. & TSIEN, R. W. (2000). Nomenclature of voltage-gated calcium channels. *Neuron* **25**, 533–535.
- GUYTON, A. C. & HALL, J. E. (1996). Chapter 18, In *The Textbook of Medical Physiology*, 9th edn, W.B. Saunders Company, Philadelphia, USA.
- HARPER, S., WEBB, T. E., CHARLTON, S. J., NG, L. L. & BOARDER, M. R. (1998). Evidence that P2Y<sub>4</sub> nucleotide receptors are involved in the regulation of rat aortic smooth muscle cells by UTP and ATP. *British Journal of Pharmacology* **124**, 703–710.
- HOFMANN, F., LACINOVA, L. & KLUGBAUER, N. (1999). Voltage-dependent calcium channels. *Reviews in Physiology, Biochemistry and Pharmacology* **139**, 33–87.
- HOLLOPETER, G., JANTZEN, H.-M., VINCENT, D., LI, G., ENGLAND, L., RAMAKRISHNAN, V., YANG, R.-B., NURDEN, P., NURDEN, A., JULIUS, D. & CONLEY, P. B. (2001). Identification of the platelet ADP receptor targeted by antithrombotic drugs. *Nature* **409**, 202–207.
- HORIUCHI, T., DIETRICH, H. H., TSUGANE, S. & DACEY, R. G. JR. (2001). Analysis of purine- and pyrimidine-induced vascular responses in the isolated rat cerebral arteriole. *American Journal of Physiology – Heart and Circulatory Physiology* **280**, H767–776.
- INOUE, R. & ITO, Y. (2000). Intracellular ATP slows time-dependent decline of muscarinic cation current in guinea pig ileal smooth muscle. *American Journal of Physiology – Cell Physiology* **279**, C1307–1318.
- JACOBSON, K. A., KING, B. F. & BURSTOCK, G. (2000). Pharmacological characterization of P2 (nucleotide) receptors. *Cell transmissions* **16**, 3–16.
- KANEKO, S., AKAIKE, A. & SATOH, M. (1999). Receptor-mediated modulation of voltage-dependent Ca<sup>2+</sup> channels via heterotrimeric G-proteins in neurones. *Japanese Journal of Pharmacology* **81**, 324–331.
- KENNEDY, C. & LEFF, P. (1995). How should P2X prinoceptors be classified pharmacologically? *Trends in Pharmacological Sciences* **16**, 168–174.
- KING, B. F., TOWNSEND-NOCHOLSON, A. & BURSTOCK, G. (1998). Metabotropic receptors for ATP and UTP: exploring the correspondence between native and recombinant nucleotide receptors. *Trends in Pharmacological Sciences* **19**, 506–514.

- KUNAPULI, S. P. & DANIEL, J. L. (1998). P2 receptor subtypes in the cardiovascular system. *Biochemical Journal* **336**, 513–523.
- KURIYAMA, H., KITAMURA, K., ITOH, T. & INOUE, R. (1998). Physiological features of visceral smooth muscle cells, with special reference to receptors and ion channels. *Physiological Reviews* **87**, 811–920.
- LAGAUD, G. J. L., STOCLET, J. C. & ANDRIANTSITOHAINA, R. (1996). Calcium handling and purinoceptor subtypes involved in ATP-induced contraction in rat small mesenteric arteries. *Journal of Physiology* **492**, 689–703.
- LEWIS, C. J., ENNION, S. J. & EVANS, R. J. (2000). P2 purinoceptor-mediated control of rat cerebral (pial) microvasculature; contribution of P2X and P2Y receptors. *Journal of Physiology* **527**, 315–324.
- MIYAGI, Y., KOBAYASHI, S., NISHIMURA, J., FUKUI, M. & KANAIDE, H. (1996). Dual regulation of cerebrovascular tone by UTP: P2U receptor-mediated contraction and endothelium-dependent relaxation. *British Journal of Pharmacology* **118**, 847–856.
- MORITA, H., COUSINS, H., ONOUE, H., ITO, Y. & INOUE, R. (1999). Predominant distribution of nifedipine-insensitive, high voltage-activated Ca<sup>2+</sup> channels in the terminal mesenteric artery of guinea pig. *Circulation Research* **85**, 596–605.
- MORITA, H., INOUE, R. & ITO, Y. (2000). Dual regulation by ATP through P2Y receptors of a novel nifedipine-insensitive (NI), high voltage-activated (HVA) Ca<sup>2+</sup> channel in guinea-pig mesenteric arteriole smooth muscle cells. *Japanese Journal of Pharmacology* **82**, 82P.
- MUTAFOVA-YAMBOLIEVA, V. N., CAROLAN, B. M., HARDEN, T. K. & KEEF, K. D. (2000). Multiple P2Y receptors mediate contraction in guinea pig mesenteric vein. *General Pharmacology* **34**, 127–136.
- NELSON, M. T., PATLAK, J. B., WORLEY, J. F. & STANDEN, N. B. (1990). Calcium channels, potassium channels, and voltage-dependence of arterial smooth muscle tone. *American Journal of Physiology* **259**, C3–18.
- RUBINO, A. & BURSTOCK, G. (1996). Evidence for a P2-purinoceptor mediating vasoconstriction by UTP, ATP and related nucleotides in the isolated pulmonary vascular bed of the rat. *British Journal of Pharmacology* **118**, 1415–1420.
- STARKE, K. (1991). Noradrenaline-ATP co-transmission in the sympathetic nervous system. *Trends in Pharmacological Sciences* **12**, 319–324.
- SURPRENANT, A., BUELL, G. & NORTH, R. A. (1995). P2X receptors bring new structure to ligand-gated ion channels. *Trends in Pharmacological Sciences* **18**, 224–229.
- THAPALIYA, S., MATSUYAMA, H. & TAKEWAKI, T. (1999). ATP released from perivascular nerves hyperpolarizes smooth muscle cells by releasing an endothelium-derived factor in hamster mesenteric arteries. *Journal of Physiology* **521**, 191–199.

### Acknowledgements

We would like to thank Professor A. F. Brading, University Department of Pharmacology, Oxford, for critical reading of our manuscript. H. M. is a research fellow of the Japanese Society for the Promotion of Sciences. This work is supported by a grant-in-aid for scientific research from the Japan Society for the Promotion of Sciences to Y. I.